

A Few Advances in Atmospheric Sciences During 2010-2014 in  
China Reported by CNC-IAMAS

Daren Lu, Rucong Yu, and Jianchun Bian

1. Development of numerical weather prediction and Climate models and their applications (by Yu, Wu, Zhou, Wang & Li)
2. Simulations of seasonal, interannual, decadal to millennium variability by climate models (by Zhou)
3. Aerosols and Climate (by Liao)
4. Radiative transfer and its numerical simulation (by Duan)
5. Stratospheric processes and stratosphere-troposphere coupling (by Bian, Lu & Chen)

# Development of numerical weather prediction and Climate models and their applications

Rucong Yu, Tongwen Wu, Tianjun Zhou, Jianjie Wang, and Jian Li

(China Meteorological Administration)

## **1. Development of numerical weather prediction (NWP) model for operation**

Since 2011, there have been noticeable improvements on the Global& Regional Assimilation and Prediction System (namely GRAPES), which is designed as a multi-scale unified NWP model with a unified non-hydrostatic dynamical core and different physics packages for various applications.

A new version of GRAPES global forecast system (GRAPES-GFS 25kmL60) is developed and under testing. The main progresses for model part include: (1) the increases in horizontal resolution from 0.5degree to 0.25 degree, and in vertical levels from 36 to 60, as well as the lifting on model top from 10hPa to about 3hPa; (2) the development of the non-interpolating SL scheme for potential temperature in upper level to improve the accuracy of model calculation; (3) introduction of a material advection scheme, the Piecewise Rational Method (PRM) into the GRAPES\_GFS, to replace the Quasi-Monotone Semi-Lagrangian (QMSL) scheme. The PRM scheme is based on a piecewise continuous rational function, solves the flux form of the water vapor equation, and treats the polar regions with a mixing technique, and can effectively improve the simulation of the advection and distribution of moisture, and the accuracy of precipitation forecasts of GRAPES-GFS as well; (4) implementation of a prognostic cloud fraction scheme by considering the contributions from macro-cloud of grid scale and the detrainment of water contents from sub-grid of cumulous, etc.

There are also lots of advancements in GRAPES-Var data assimilation, particularly on the following aspects: (1) GRAPES-3DVar has been updated to completely employ the same grids and state variables as those of the GRAPES model. The new features of GRAPES-3DVar include: the physical characteristic and location of analysis variables are consistent with those of forecast model; the balance

constraint relationship of mass and wind fields is developed on the height-based terrain-following coordinate; the preconditioning transform allows different vertical covariance for each horizontal spectral mode, giving them more control over the variations in horizontal scale with height; the observation operators are redesigned in order to match the new coordinate and grids. (2) Two key problems have been identified in bias correction: Firstly, bias corrections can drift towards unrealistic values in regions where there is strong model error (especially for developing models with not well tuned physics) and relatively few “anchor” observations, i.e., observations that have little systematic error and therefore allow the separation between model and observation bias. Secondly, there is undesired interaction between the quality control and bias correction for observations where bias-corrected observation departures are used for quality control and where these departures show skewed distributions (e.g., in case of cloud detection). Constrained Bias Correction (CBC) scheme is proposed using priori knowledge of radiometric uncertainty information in GRAPES in order to avoid the drift of observation bias correction to the biased model background. It is a kind of Tikhonov regularization techniques in inverse problems using minimum norm solution with priori information. (3) Fengyun-3 (FY-3) satellites are Chinese new generation polar-orbiting meteorological satellites. A new cloud detection algorithm is proposed for the MWTS. The method is based on the cloud fraction product provided by the Visible and Infrared Radiometer (VIRR) on board FY-3satellites. A MWTS field-of-view (FOV) with a cloud fraction greater than a threshold  $f_{VIRR}$  will be identified as a cloudy radiance. The threshold  $f_{VIRR}$  is determined by the AMSU-A cloud liquid water path products, obtained from the Microwave Surface and Precipitation Products System (MSPPS). (4) GRAPES 4D-Var is under development. The tangent linear model (TLM) and adjoint models (ADM) were rebuilt based the new GRAPES-GFS model version GRAPES-GFS 25-50km/L60, and the parallel efficiency has been improved by reducing parallel halo partition and ADM’s base state using push/pop to save memory. The new TLM and ADM greatly improved the parallel efficiency of GRAEPS Global 4D-Var.

## **2. Development of Climate models and applications in climate prediction and**

## climate change research

In recent years, five climate models developed by Chinese institutions have participated in CMIP5. These five models include (BCC\_CSM1.1 and BCC\_CSM1.1(m) developed in Beijing Climate Center, BNU-ESM developed in Beijing Normal University, FGOALS\_g2 and FGOALS\_s2 developed in the Institute of Atmospheric Physics, Chinese Academy of Sciences. More details of these models are shown in Table 1. Evaluation analyses show that the five Chinese models show reasonable performances in the simulations of climate mean state, intra-seasonal oscillation, interannual ENSO variability, global and East Asian monsoon, climate evolution of the 20th century, major teleconnections, and many other features .

In order for the forthcoming CMIP6, the new versions of BCC\_CSM, FGOALS, BNU\_ESM, FIO\_ESM in China are also under development. The improvements relative to CMIP5 versions for each model group mainly include: (a) Increased resolution and improved dynamical core for AGCM and OGCM; (b) Improved physical schemes in OGCMs, boundary layer scheme, cumulus convection, radiation, gravity waves and etc. in AGCMs; (c) Terrestrial carbon cycle and more human activity processes such as land use, anthropogenic groundwater exploitation schemes in the land components; (d) More complex atmospheric chemical processes.

**Table 1** The Chinese models used for IPCC AR5

| <b>Model name</b> | <b>Institute</b>      | <b>Horizontal resolution of atmospheric model</b> | <b>Horizontal resolution of oceanic model</b> |
|-------------------|-----------------------|---|---|
| BCC_CSM1.1        | BCC (China)           | 2.8°×2.8°   | 0.8°×1.0°                                     |
| BCC_CSM1.1(m)     | BCC (China)           | 1.1°×1.1°   | 0.8°×1.0°                                     |
| BNU-ESM           | BNU (China)           | 2.8°×2.8°   | 0.9°×1.0°                                     |
| FGOALS-g2         | IAP-LASG-CESS (China) | 3°×2.8°   | 0.9°×1.0°                                     |
| FGOALS-s2         | IAP-LASG (China)      | 1.7°×2.8°   | 0.9°×1.0°                                     |

Effort has been devoted to developing high resolution climate system model in

BCC. As one of the National Program on Key Basic Research Project, “High resolution climate system model development and evaluation” project has been implemented for five years since June 2010. The main progresses may be summarized as “two systems” and “one platform”, where “two systems” refers to the high-resolution modeling system and the model evaluation system, “one platform” to the multi-model ensemble coupling platform. Major achievements can be summarized below:

(1) A fully coupled high-resolution BCC Climate System Model (BCC\_CSM2.0) with a horizontal resolution of T266 (approximately  $45 \times 45$  km) in the atmosphere and  $30 \times 30$  km in the tropical ocean has been established. High resolution significantly benefits the reproduction of tropical cyclones and southwest vortices, and improves the spatial distribution and intensity structure of the simulated precipitation. It is developed from a lower resolution version of climate system model (BCC\_CSM). Development of the high-resolution climate system model involves the following studies: (a) Improvement of dynamic framework. Focusing on the overestimation of precipitation over steep mountains, which has been a long-lasting bias in many climate models, a finite-difference approach for trace transport algorithm (the two-step shape preserving scheme, TSPAS) and a new leaping-point difference method have been employed in climate models. The modified model restrains the “overshoot” of water vapor to the high-altitude region of the windward slopes and significantly reduces the overestimation of precipitation in areas above 2000 m along the southern edge of the Tibetan Plateau. (b) Improvement of model physics includes: The parameterization scheme for mass-flux-type cumulus convection, which is based on a bulk-cloud approach with its own unique properties, especially for the treatment of convective updrafts and downdrafts, has been improved and employed in climate models; Gravity waves generated by all major sources, including convection and geostrophic adjustment, are involved in new schemes; Humidity-based cloud fraction parameterization has been improved; A new scheme for sensible and latent heat fluxes from the ocean surface has been implemented; The land surface process scheme has been updated.

(2) An ensemble coupler platform is set up through the ensemble of momentum,

energy, and water fluxes simultaneously interacting with several different atmosphere model components in a climate model system. The simulations using the ensemble with several different AGCM in this platform can partly improve the ENSO and the basic mean climate of SST. The experiment using the ensemble of the same version of AGCM with several different atmospheric initial conditions is also carried out. It may filter the atmospheric noise. This ensemble method is useful for understanding impacts of the atmospheric noise on simulations of the global climate and ENSO.

(3) A system to evaluate climate model is basically built. The evaluative criteria for climate mean state and East Asian monsoon are suggested and preliminary evaluation scheme has basically been proposed. (a) The evaluations for the performances of several climate models and different model physics processes and parameters have been carried out. The results show that some high resolution models have better performances than those with relatively low resolution. (b) Innovative method to evaluate the evolvments and process characteristics of rainfall events in East Asia is proposed. It is designed by compositing rainfall events centered at the maximum moment of each event and a regional rainfall coefficient to quantify the spatiotemporal variation of rainfall events.

In addition to the development of climate system models, achievement has been made in developing operational climate prediction system in BCC. In 2014, the second-generation short-range climate forecast system using BCC Climate System Model in National Climate Center, CMA is established. It is composed of three sub-systems, i.e. the global ocean data assimilation system, the monthly-scale extended-range dynamic forecast system, and the seasonal climate forecast system. With better assimilations of temperature and salinity, the second-generation ocean data assimilation system is now at the quasi-operational level. The atmospheric general circulation model BCC\_AGCM2.2 and the climate system model BCC\_CSM1.1(m) are the main tools for the second-generation monthly-scale extended-range dynamic forecast system and the second-generation seasonal prediction system, respectively. The former entered into operational use in 2013, and the latter entered into its operational stage in 2014. A preliminary evaluation indicates that the second-generation system shows a certain

capability in predicting the pentad, ten-day, monthly, seasonal and interannual climate variability. It exhibits a higher prediction skill, compared to the first-generation system, in terms of precipitation, surface air temperature and atmospheric circulation.

Besides the newly version of fully coupled climate system model BCC-CSM2 with the medium resolution of T106 and 40 layers in atmosphere, the BCC Climate Prediction System (BCC-CPS) is also developing. The version of BCC-CPS1.0 has been involved in the recent sub-seasonal to seasonal (S2S) Prediction Project, and 20-years of 0-60 days lead time forecast data from May 1995 to April 2014 have been produced. The project bridges the gap between weather and climate and can help us to improve forecast skill and understanding on the sub-seasonal to seasonal timescale with special emphasis on high-impact weather events. It also promotes the initiative's uptake by operational centers and exploitation by the applications community, and capitalizes on the expertise of the weather and climate research communities to address issues of importance to the Global Framework for Climate Services.

### **3. Advances in analyses of rainfall process**

Innovative methods are proposed to investigate the fine evolvments and processes characteristics of rainfall events: (1) a method to analyze the evolution of the rainfall process is designed by compositing rainfall events centered at the maximum moment of each event; (2) a regional rainfall coefficient (RRC) is defined to quantify the spatiotemporal variation of rainfall events. These studies present an effort to explore more complete spatiotemporal organization and evolution of rainfall events. The results reveal that the rainfall process is asymmetric, which means rainfall events usually reach the maximum in a short period and then experience a relatively longer retreat to the end of the event. The asymmetry in short-duration rainfall is more obvious than that in long-duration rainfall, and the rainfall events that reach the maximum during 1400–0200 LST exhibit the strongest asymmetry. It is also found that the asymmetry is more obvious in rainfall events with strong intensity and over areas with complex terrain such as Southwestern China. Using the regional rainfall coefficient (RRC), the differences of rainfall intensity and duration time between local and regional rainfall events are revealed. It is found that the RRC reaches a maximum

a few hours after the peak intensity was reached, implying the development of cloud anvil and stratiform precipitation after the peak of convections.

To further expanding the understanding of physical mechanisms underlying the rainfall variability, several new observation phenomena have been demonstrated under the background of inter-decadal rainfall changes known as the so-called “southern flooding and northern drought” (SFND) pattern over eastern China in recent decades. It is found that although the rainfall amount and frequency have significantly increased (decreased) in the mid–lower reaches of the Yangtze River valley (North China), the rainfall intensity has decreased (increased). Results also show that the SFND pattern is mostly attributed to changes in precipitation with moderate and low intensity, while the high intensity precipitation does not show a significant SFND pattern. Further analyses indicate that the duration-related rainfall structure also experienced significant changes. The “northern drought” can be partly ascribed to the decreases of long duration rainfall in the night and early morning. The “southern flooding” is contributed by both the increases of late afternoon rainfall with short and medium duration and early morning rainfall with long duration.

### **Main references**

- Bao, Q., and Coauthors, 2013: The Flexible Global Ocean-Atmosphere-Land System Model, Spectral Version 2: FGOALS-s2. *Adv. Atmos. Sci.*, 30, 561–576, doi: 10.1007/s00376-012-2113-9.
- Li, L. J., and Coauthors, 2013: The Flexible Global Ocean-Atmosphere-Land System Model: Grid-point Version 2: FGOALS-g2. *Adv. Atmos. Sci.*, 30, 543–560, doi: 10.1007/s00376-012-2140-6.
- Li, J., R.C. Yu, W.H. Yuan, H.M. Chen, 2011: Changes in duration-related characteristics of late-summer precipitation over eastern China in the past 40 years. *J. Climate*, 24(21), 5683-5690.
- Li, Juan, and X. Zou, 2013: A quality control procedure for FY-3A MWTS measurements with emphasis on cloud detection using VIRR cloud fraction. *J. Atmos. Oceanic Technol.*, 30, 1704–1715.
- Liu, Y. and J.S. Xue, 2014: Operational implementation of the assimilation of global navigation

- satellite radio occultation observations into the GRAPES data assimilation system, *Journal of Meteorological Research* DOI: 10.1007/s13351-014-4028-0.
- Su, Y., X.S. Shen, X.D. Peng, and Coauthors, 2013: Application of PRM scalar advection scheme in GRAPES global forecast system. *Chinese Journal of Atmospheric Sciences (in Chinese)*, 37 (6): 1309–1325.
- Vitart, F., A. W. Robertson, and D. L. T. Anderson, 2012: Subseasonal to Seasonal Prediction Project: bridging the gap between weather and climate. *WMO Bulletin*, 61(2), 23--28.
- Wang, R.C., J.D. Gong, L. Zhang, and Coauthors, 2014: Tropical balance characteristics between mass and wind fields and their impact on analyses and forecasts of GRAPES. Part I: Balance characteristics. *Chinese Journal of Atmospheric Sciences (in Chinese)*, doi:10.3878/j.issn.1006-9895.1412.14233. (In Press)
- Wu, T. W., 2012: A mass-flux cumulus parameterization scheme for large-scale models: description and test with observations. *Clim. Dyn.*, 38, 725-744.
- Wu, T. W., and Coauthors, 2013a: Global carbon budgets simulated by the Beijing climate center climate system model for the last century. *J. Geophys. Res. Atmos.*, 118, 4326--4347, doi: 10.1002/jgrd.50320.
- Wu, T. W., and Coauthors, 2013b: Progress in developing the Short-range operational climate prediction system of China National Climate Center. *J. Applied Meteor. Sci.*, 24(5), 533--543 (in Chinese)
- Wu, T. W., and Coauthors, 2014: An overview of BCC climate system model development and application for climate change studies. *J. Meteor. Res.*, 28(1), 34--56.
- Wu, Q. Z., and Coauthors, 2013: Introduction of the CMIP5 experiments carried out by BNU-ESM. *Advances in Climate Change Research*, 9(4), 291–294. (in Chinese)
- Xin, X.G., T. W. Wu, J. Zhang, 2012: Introduction of CMIP5 experiments carried out by BCC climate system model. *Advances in Climate Change Research*, 8(5), 378-382 (in Chinese).
- Xue, J.S., and D.H. Chen: Scientific design and application of GRAPES (in Chinese), Science press, 2008.
- Xue, J.S., Y. Liu, and L. Zhang: Scientific documentation of GRAPES-3DVar system for the global model (in Chinese), Numerical Weather Prediction Center, China Meteorological Administration, 2012.

- Yu, R.C., W. Yuan, and J. Li, 2013: The asymmetry of rainfall process. *Chinese Science Bulletin*, 58(16), 1850-1856.
- Yu, R.C., J. Li, W.H. Yuan, H.M. Chen, 2010: Changes in Characteristics of Late-Summer Precipitation over Eastern China in the Past 40 Years Revealed by Hourly Precipitation Data. *Journal of Climate*, 23(12), 3390–3396.
- Yu, R.C., J. Li, Y. Zhang, H.M. Chen, 2015: Improvement of rainfall simulation on the steep edge of the Tibetan Plateau by using a finite difference transport scheme in CAM5. *Climate Dynamics*, DOI 10.1007/s00382-015-2515-3.
- Yu R.C., H. Chen, W. Sun, 2015, Definition and characteristics of regional-rainfall-events demonstrated by warm season precipitation over the Beijing plain, *Journal of Hydrometeorology*, Vol. 1, 396-406.
- Zhou T.J., X.L. Chen, L. Dong, and Coauthors, 2014: Chinese contribution to CMIP5: An overview of five Chinese models' performances. *J. Meteor. Res.*, 28(4), 481–509.
- Zhou T.J., and Coauthors, 2014: Development of earth/climate system models in China: A review from the Coupled Model Intercomparison Project perspective. *J. Meteor. Res.*, 28(5), 762-779.

# Simulations of seasonal, interannual, decadal to millennium variability by climate models

Tianjun Zhou

(LASG, Institute of Atmospheric Physics, Chinese Academy of Sciences)

## 1. The simulation of western North Pacific Subtropical High (WNPSH)

The WNPSH is characterized by two distinct interannual variability modes. In order to clarify the relationship between these two modes and SST forcing, He and Zhou (2014) have evaluated the performance of the CMIP5-AMIP models on these two modes. The CMIP5-AMIP models, which are forced by the historical SST, perform well in simulating the first mode. The CMIP5-AMIP models also well capture the forcing mechanisms for the second mode, including the influence from tropical Indian Ocean through Kelvin wave, the influence from the maritime continent by local Hadley circulation anomaly, and the influence from the equatorial central Pacific through Rossby wave. These evidences suggest the first mode is an SST forced phenomenon. In contrast, the second mode is only partially reproduced by the CMIP5-AMIP models. Among the five years associated with the second mode, the WNPSH anomalies are reproduced by the CMIP5-AMIP models in only two years. The local negative relationship between the anomalous anticyclone and the SST anomaly for the second mode is not reproduced by the CMIP5-AMIP models. These evidences suggest that the second mode cannot be explained as an SST forced phenomenon. The above results have improved our understanding on the mechanism for the interannual variability of the WNPSH.

The WNPSH has great influence on the climate of eastern China in summer. The mechanisms for the interannual and intraseasonal variability of WNPSH have been well studied, but it is still unknown how the intensity of the WNPSH will change in response to global warming. He and Zhou (2015) investigated the projected changes of the WNPSH using the RCP4.5 and RCP8.5 warming scenarios of 33 CMIP5

models. The results show that the projected changes in the WNPSH intensity is *highly inconsistent* among the models. About half of the models project enhanced WNPSH and about half of the models project weakened WNPSH, under both RCP4.5 and RCP8.5 scenarios. The multi-model ensemble mean (MME) projects little change in the WNPSH intensity. Further investigation on the inter-model spread shows that the projected changes in the WNPSH intensity depends on the change of the zonal SST gradient in the tropical oceans. Stronger (weaker) warming of the tropical Indian Ocean than the tropical western Pacific Ocean is in favor of an enhanced (weakened) WNPSH in the projection. The rainfall pattern in eastern China is regulated by the changes in the WNPSH intensity. Models with an enhanced (weakened) WNPSH are associated with increased precipitation over the northern (southern) part of eastern China, accompanied by enhanced (weakened) southerly wind.

## **2. The simulation of large-scale atmospheric circulation in the RCP4.5 and mid-Pliocene (MP).**

The MP warm period (~3.3–3.0 Ma) is often considered as the last sustained warm period with close enough geographic configurations compared to the present one associated with atmospheric CO<sub>2</sub> concentration (405±50 ppm) higher than the modern level. For this reason, this period is often considered as a potential analogue for the future climate warming, with the mean global surface air temperatures (SAT) are estimated to be 2–3°C above pre-industrial. RCP4.5 scenario features the similar SAT warming amplitude with MP, thus it has been selected to compare the pattern of tropical atmospheric response with the MP. Our results show that there is a damping of the Hadley cell intensity in the northern tropics and an increase in both subtropics associated with northern and southern Hadley cells poleward expansion. The response of the Hadley cells is stronger for the RCP4.5 scenario than for the MP, but in very good agreement with the fact that the atmospheric CO<sub>2</sub> concentration is higher in the future scenario than in the mid-Pliocene (543 versus 405 ppm). Concerning the response of the Walker cell, we show that despite very large similarities, there are also some differences. Common features to both scenarios are: weakening of the ascending

branch, leading to a suppression of the precipitation over the western tropical Pacific. The response of the Walker cell is stronger in the RCP4.5 scenario than in the MP but also depicts some major differences, as an eastward shift of its rising branch in the future scenario compared to the MP. In this paper, we explain the dynamics of the Hadley and Walker cells, and show that despite a minor discrepancy, the MP is certainly an interesting analogue for future climate changes in tropical areas (Sun et al. 2013).

### **3. The simulation of seasonal precipitation changes over the globe**

Seasonal precipitation changes over the globe during the 20th century simulated by two versions of the Flexible Global Ocean–Atmosphere–Land System (FGOALS) model are assessed (Ma and Zhou 2015). The analysis of globally averaged seasonal precipitation changes show that wet seasons get wetter and the annual range (precipitation difference between wet and dry seasons) increases during the 20th century in the two models, with positive trends covering most parts of the globe, which is consistent with observations. However, both models show a moistening dry season, which is opposite to observations. Analysis of the globally averaged moisture budget in the historical simulations of the two models shows little change in the horizontal moisture advection in both the wet and dry seasons. The globally averaged seasonal precipitation changes are mainly dominated by the changes in evaporation and vertical moisture advection. Evaporation and vertical moisture advection combine to make wet seasons wetter and enhance the annual range. In the dry season, the opposite change of evaporation and vertical moisture advection leads to an insignificant change in precipitation. Vertical moisture advection is the most important term that determines the changes in precipitation, wherein the thermodynamic component is dominant and the dynamic component tends to offset the effect of the thermodynamic component.

### **4. The simulation of tropical Pacific Walker circulation (WC)**

The tropical Pacific WC in the two versions of FGOALS is evaluated (Ma and

Zhou 2014). Observed Indo-Pacific sea level pressure (SLP) reveals a reduction of WC during 1900–2004 and 1950–2004, and an enhancement of WC during 1982–2004. During the three different time spans, the WC in FGOALS-g2 shows a weakening trend. In FGOALS-s2, tropical Pacific atmospheric circulation shows no significant change over the past century, but the WC strengthens during 1950–2004 and 1982–2004. The change of WC is explained by the hydrological cycle constraints that precipitation must be balanced with the moisture transporting from the atmospheric boundary layer to the free troposphere. In FGOALS-g2, the increasing amplitude of the relative variability of precipitation is smaller (larger) than the relative variability of moisture over the tropical western (eastern) Pacific over the three time spans, and thus leads to a weakened WC. In FGOALS-s2, the convective mass exchange fluxes increase (decrease) over the tropical western (eastern) Pacific over 1950–2004 and 1982–2004, and thus leads to a strengthened WC. The distributions of sea surface temperature (SST) trends dominate the change of WC. Over 1950–2004 and 1982–2004, tropical Pacific SST shows an El Niño-like (La Niña-like) trend pattern in FGOALS-g2 (FGOALS-s2), which drives the weakening (strengthening) of WC. Therefore, a successful simulation of the tropical Pacific SST change pattern is necessary for a reasonable simulation of WC change in climate system models.

## **5. The simulation of East Asian summer monsoon (EASM)**

The inter-annual variability of EASM is investigated in 13 CMIP3 and 19 CMIP5 atmospheric models (Song and Zhou 2014a). The skill origin is found to be rooted in the Indian Ocean-western Pacific anticyclone (IO-WPAC) teleconnection. In the high-skill models, the tropical eastern Indian Ocean warming leads to the positive precipitation anomalies. The released heat induces the atmospheric Kelvin wave response and maintains the western Pacific anticyclone. In the low-skill models, these processes are not captured well.

Further, 17 CMIP5 atmospheric and corresponding coupled models are compared to clarify the role of air-sea interaction in the EASM (Song and Zhou 2014). Both the climatology and inter-annual variability simulation of EASM are improved

through the air-sea interaction. For the climatology, the local cold SST biases in the coupled models reduce the surface evaporation and intensify the western Pacific subtropical high. For the inter-annual variability, the air-sea interaction intensifies the IO-WPAC teleconnection and enhances the EASM simulation.

The responses of EASM to natural and anthropogenic forcings are examined in the 17 latest CMIP5 models with 105 realizations (Song et al. 2014). The observed weakening trend of EASM circulation during 1958-2001 is partly reproduced under all-forcing runs. A comparison of separate forcing experiments reveals that the aerosol-forcing plays a primary role in driving the weakened monsoon circulation. The preferential cooling over continental East Asia caused by aerosol affects the monsoon circulation through reducing the land-sea thermal contrast and results in higher sea level pressure over northern China.

## **6. The simulation of Indian Ocean sea surface temperature (SST)**

The mechanism responsible for Indian Ocean Sea surface temperature (SST) basin-wide warming trend during 1958-2004 is studied based on numerical experiments based on LASG/IAP climate system model FGOALS-gl (all forcing run, natural forcing run, pre-industrial control run). The results show that the warming during 1958-2004 (0.5 K) is largely attributed to the external forcing, especially anthropogenic forcing (Dong et al. 2014a). Anthropogenic forcing mainly includes greenhouse gases (GHGs) and anthropogenic aerosols (AAs). The individual roles of GHGs and AAs on the warming of the Indian Ocean and the evolution of Pacific Decadal Variability (PDV) during the twentieth century are investigated using CMIP5 models. The increasing GHGs are considered to be one reason for the Indian Ocean warming. Model evidence is provided that the emission of AAs has slowed down the warming rate at 0.34 K per century, mainly through its indirect effect. GHGs and AAs have competed with each other in forming the basin-wide warming pattern as well as the equatorial East-West dipole warming pattern in the Indian Ocean (Dong and Zhou 2014). Evidence also shows that PDV phase transition is dominated by internal variability, but it is also significantly affected by external forcing. The combined

effects of GHGs and AAs favor the positive phase of PDV with stronger ocean warming in the tropics than the extratropical Pacific (Dong et al. 2014b).

## **7. The climate simulation by a Regional Ocean-Atmosphere Coupled Model (ROAM)**

The ROAM is an important tool for understanding the impacts of regional air-sea interactions on the monsoon variability, and for the dynamical downscaling of the global climate model. A regional ocean-atmosphere coupled model was developed in LASG, which is named as FROALS (Flexible Regional Ocean-Atmosphere-Land System model) (Zou and Zhou 2012, 2014). The major advantage of FROALS is that it consists of two atmospheric model components and two oceanic model components. By using this flexible model system, the effects of different atmospheric model components and different oceanic model components on the ROAM simulations over western North Pacific are investigated. Results suggest that simulated biases in FROALS are mainly contributed from the atmospheric model component (Zou and Zhou 2012, 2014). The cold biases of simulated sea surface temperature in FROALS are significantly reduced when the convection suppression criterion is applied (Zou and Zhou 2011). The advanced FROALS shows reasonable performance over western North Pacific. The climatology and interannual variability of surface current over western North Pacific are well captured. Compared with the uncoupled simulation, the regionally coupled simulation exhibits improvements in the interannual variability of rainfall and tropical cyclone genesis potential index over the WNP (Zou and Zhou 2013). Finally, the FROALS is used to dynamically downscale the present-day climate simulation and future climate projections of a global climate system model. The preliminary analysis indicate that the regional climate over East Asia derived from FROALS is better than those derived from global climate model and the uncoupled regional model, indicating that the FROALS has good application prospects over this region.

## **7. The simulation of the last millennium.**

To achieve a better understanding of the 20th century global warming, we need to extend our study from the past century to the past millennium (Zhou et al. 2009). Recent work reports the last millennial climate simulated by the climate system model FGOALS-g1 of Chinese Academy of Sciences (Man and Zhou 2014a). Major features of the simulated temperature variations over China, including the Medieval Climate Anomaly (MCA), the Little Ice Age (LIA) and the present warming stage over the 20th century, are generally consistent with the reconstructions. The centennial East Asian summer monsoon (EASM) variations exhibit a stronger monsoon circulation during the MCA than that during the LIA (Man et al. 2012). The land-sea thermal contrast change caused by the effective radiative forcing lead to the MCA and LIA monsoon changes. The cooling over the middle-high latitudes of the East Asian continent is stronger than that over the tropical ocean after large volcanic eruptions. This temperature anomaly pattern favors a weaker EASM circulation (Man et al. 2014b, c). A comparison of inter-annual variability mode of EASM rainfall during the MCA, LIA and 20CW reveals a similar rainfall anomaly pattern. But the time periods of the leading inter-annual variability mode during three typical time periods of the last millennium are different, and the biannual oscillation is most evident during the warm period (Zhou et al. 2011).

## References

1. Dong Lu, Tianjun Zhou and Bo Wu, 2014a: Indian Ocean warming during 1958-2004 simulated by a climate system model and its mechanism. *Clim. Dyn.*, 42: 203-217, doi: 10.1007/s00382-013-1722-z.
2. Dong, Lu, and Tianjun Zhou, 2014: The Indian Ocean Sea Surface Temperature Warming Simulated by CMIP5 Models during the 20th Century: Competing Forcing Roles of GHGs and Anthropogenic Aerosols. *Journal of Climate*, 27, 3348–3362.
3. Dong Lu, Tianjun Zhou and Xiaolong Chen, 2014b: Changes of Pacific Decadal Variability in the Twentieth Century Driven by Internal Variability, Greenhouse Gases and Aerosols. *Geophys. Res. Lett.*, 41, DOI: 10.1002/2014GL062269.

4. He, C., and T. Zhou, 2014: The two interannual variability modes of the Western North Pacific Subtropical High simulated by 28 CMIP5–AMIP models. *Clim Dynam*, **43**, 2455-2469.
5. He, C., and T. Zhou, 2015: Responses of the Western North Pacific Subtropical High to Global Warming under RCP4.5 and RCP8.5 Scenarios Projected by 33 CMIP5 Models: The Dominance of Tropical Indian Ocean–Tropical Western Pacific SST Gradient. *J Climate*, **28**, 365-380.
6. MA Shuangmei and ZHOU Tianjun, 2015: Precipitation Changes in Wet and Dry Seasons over the 20th Century Simulated by Two Versions of the FGOALS Model. *Adv. Atmos. Sci.*, in press.
7. Ma S M, Zhou T J. 2014. Changes of the tropical Pacific Walker circulation simulated by two versions of FGOALS model. *Science China: Earth Sciences*, doi: 10.1007/s11430-014-4902-8.
8. Man, W., and T. Zhou, 2014a: Regional-scale surface air temperature and East Asian summer monsoon changes during the last millennium simulated by the FGOALS-gl Climate System Model. *Adv. Atmos. Sci.*, 31(4), 765-778, doi: 10.1007/s00376-013-3123-y.
9. Man, W., T. Zhou, and J. Jungclaus, 2014b: Effects of large volcanic eruptions on global summer climate and East Asian monsoon changes during the last millennium: analysis of MPI-ESM simulations. *J. Climate*, 27(19), 7394-7409, doi: 10.1175/JCLI-D-13-00739.1.
10. Man, W., and T. Zhou, 2014c: Response of the East Asian summer monsoon to large volcanic eruptions during the last millennium. *Chin. Sci. Bull.*, 59, 4123-4129, doi: 10.1007/s11434-014-0404-5.
11. Man, W., T. Zhou, and J. Jungclaus, 2012: Simulation of the East Asian summer monsoon during the last millennium using MPI-M Earth System Model. *J. Climate*, 25(22), 7852-7866, doi: 10.1175/JCLI-D-11-00462.1.
12. Zhou, T., W. Man, and J. Zhang, 2009: Progress in numerical simulations of the climate over the last millennium. *Advances in Earth Science*, 24(5), 469-476. (in Chinese)

13. Zhou, T., B. Li, W. Man, et al. 2011: A Comparison of the Medieval Warm Period, Little Ice Age and 20th Century Warming simulated by the FGOALS Climate System Model. *Chin. Sci. Bull.*, 56, 3028-3041, doi: 10.1007/s11434-011-4641-6.
14. Song, F., and T. Zhou, 2014a: Interannual Variability of East Asian Summer Monsoon Simulated by CMIP3 and CMIP5 AGCMs: Skill Dependence on Indian Ocean–Western Pacific Anticyclone Teleconnection. *J. Climate*, 27, 1679-1697.
15. Song, F., and T. Zhou, 2014b: The climatology and inter-annual variability of East Asian summer monsoon in CMIP5 coupled models: Does air-sea coupling improve the simulations? *J. Climate*, 27, 8761–8777.
16. Song, F., T. Zhou, and Y. Qian, 2014: Responses of East Asian summer monsoon to natural and anthropogenic forcings in the 17 latest CMIP5 models. *Geophys. Res. Lett.*, 41, doi: 10.1002/2013GL058705.
17. Sun Y., G. Ramstein, C. Contoux, and T. Zhou, 2013: A comparative study of large-scale atmospheric circulation in the context of a future scenario (RCP4.5) and past warmth (mid-Pliocene), *Clim. Past*, 9, 1613-1627, doi:10.5194/cp-9-1613-2013.
18. Zou L, and Zhou T. 2011. Sensitivity of a regional ocean-atmosphere coupled model to convection parameterization over western North Pacific. *J. Geophys. Res.*, 116, D18106, doi: 10.1029/2011JD015844
19. Zou Liwei, Zhou Tianjun. 2012. Development and evaluation of a regional ocean-atmosphere coupled model with focus on the western North Pacific summer monsoon simulation: Impacts of different atmospheric components. *Sci. China Earth Sci.*, 55: 802-815
20. Zou L, and Zhou T. 2013. Can a regional ocean-atmosphere coupled model improve the simulation of the interannual variability of the western North Pacific summer monsoon? *J. Climate*, 26: 2353-2367
21. Zou L, and Zhou T. 2014. Simulation of the western North Pacific summer monsoon by regional ocean-atmosphere coupled model: Impacts of oceanic components[J]. *Chin. Sci. Bull.*, 59(7): 662-673

# Aerosols and Climate

Hong Liao

(LAPC, Institute of Atmospheric Physics, Chinese Academy of Sciences)

## 1. Measurements of aerosols

Based on a network of field stations belonging to the Chinese Academy of Sciences (CAS), the “Campaign on atmospheric Aerosol REsearch” network of China (CARE-China) (Figure 1) was recently established as the country’s first monitoring network for the study of the spatiotemporal distribution of aerosol physical characteristics, chemical components and optical properties, as well as aerosol gaseous precursors. The network comprises 36 stations in total and adopts a unified approach in terms of the instrumentation, experimental standards and data specifications. This ongoing project is intended to provide an integrated research platform to monitor online PM<sub>2.5</sub> concentrations, nine-size aerosol concentrations and chemical component distributions, nine-size secondary organic aerosol (SOA) component distributions, gaseous precursor concentrations (including SO<sub>2</sub>, NO<sub>x</sub>, CO, O<sub>3</sub> and VOCs), and aerosol optical properties. The data will be used to identify the sources of regional aerosols, the relative contributions from nature and anthropogenic emissions, the formation of secondary aerosols, and the effects of aerosol component distributions on aerosol optical properties. The results will reduce the levels of uncertainty involved in the quantitative assessment of aerosol effects on regional climate and environmental changes, and ultimately provide insight into how to mitigate anthropogenic aerosol emissions in China. Xin et al. (2015) provides a detailed description of the instrumentation, methodologies and experimental procedures used across the network, as well as a case study of observations taken from one station and the distribution of main components of aerosol over China during 2012.



nitrate, ammonium, black carbon, and organic carbon) were simulated to have the largest IAVs over NC in DJF, corresponding to the large variations in meteorological parameters over NC in this season. Process analyses were performed to identify the key meteorological parameters that determined the IAVs of different aerosol species in different regions. While the variations in temperature and specific humidity, which influenced the gas-phase formation of sulfate, jointly determined the IAVs of sulfate over NC in both DJF and JJA, wind (or convergence of wind) in DJF and precipitation in JJA were the dominant meteorological factors to influence IAVs of sulfate over SC and the SCB. The IAVs in temperature and specific humidity influenced gas-to-aerosol partitioning, which were the major factors that led to the IAVs of nitrate aerosol in China. The IAVs in wind and precipitation were found to drive the IAVs of organic carbon aerosol. We also compared the IAVs of aerosols simulated with variations in meteorological parameters alone with those simulated with variations in anthropogenic emissions alone; the variations in meteorological fields were found to dominate the IAVs of aerosols in northern and southern China over 2004–2012. Considering that the IAVs in meteorological fields are mainly associated with natural variability in the climate system, the IAVs in aerosol concentrations driven by meteorological parameters have important implications for the effectiveness of short-term air quality control strategies in China.

### **3. Climatic effect of aerosols in China**

To understand the representation of aerosols in China in current global climate models, we evaluate extensively the simulated present-day aerosol concentrations and aerosol optical depth (AOD) over China from the 12 models that participated in Atmospheric Chemistry & Climate Model Intercomparison Project (ACCMIP), by using ground-based measurements and satellite remote sensing. Ground-based measurements of aerosol concentrations used in this work include those from the CARE-China network and the China Meteorological Administration (CMA) Atmosphere Watch Network (CAWNET) as well as the observed fine-mode aerosol concentrations collected from the literature. The ground-based measurements of AOD

in China are taken from the AERosolROboticNETwork (AERONET), the sites with CIMEL sun photometer operated by Institute of Atmospheric Physics, Chinese Academy of Sciences, and from Chinese Sun Hazemeter Network (CSHNET). We find that the ACCMIP models generally underestimate concentrations of all major aerosol species in China. On an annual mean basis, the multi-model mean concentrations of sulfate, nitrate, ammonium, black carbon, and organic carbon are underestimated by 63%, 73%, 54%, 53%, and 59% (Figure 2), respectively. The multi-model mean AOD values show low biases of 20-40% at studied sites in China. The ACCMIP models can reproduce seasonal variation of nitrate but cannot capture well the seasonal variations of other aerosol species. Our analyses indicate that current global models generally underestimate the role of aerosols in China in climate simulations.

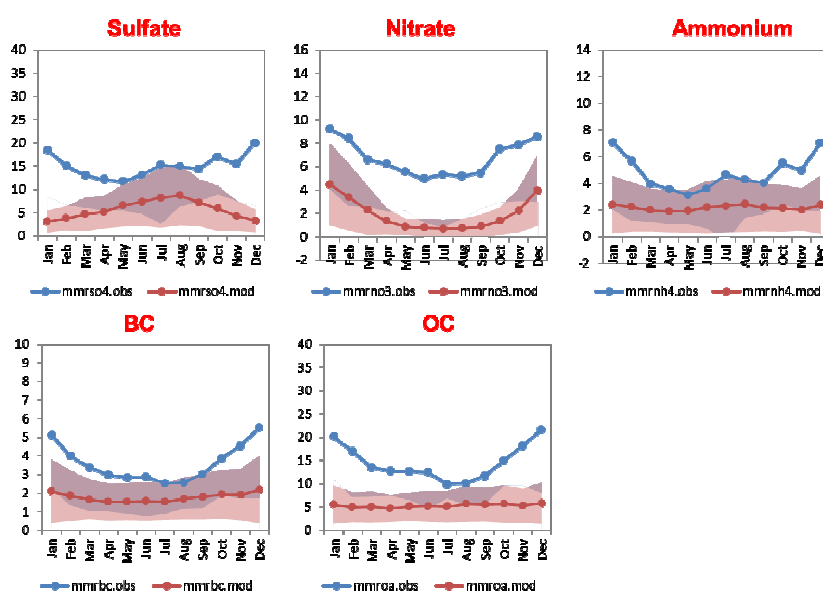


Figure 2. Comparisons of the ACCMIP multi-model mean aerosol concentrations (red lines) with ground-based measurements (blue lines).

## References:

1. Jinyuan Xin; Yuesi Wang, Yuepeng Pan, Dongsheng Ji; Zirui Liu; Tianxue Wen; Yinghong Wang; Xingru Li; Yang Sun; Jie Sun; Pucai Wang; Gehui Wang; Xinming Wang; Zhiyuan Cong; Tao Song; Lili Wang; Guiqian Tang; Wenkang Gao; Yuhong Guo; Hongyan Miao; Shili Tian; Lu Wang, The Campaign on

atmospheric Aerosol REsearch network of China: CARE-China. Bulletin of the American Meteorological Society, 2014, DOI: BAMS-D-14-00039.1.

2. Mu Q., and H. Liao, Simulation of the interannual variations of aerosols in China: Role of variations in meteorological parameters, *Atmos. Chem. Phys.*, 14, 9597-9612, doi:10.5194/acp-14-9597-2014, 2014.

# Radiative transfer and its numerical simulation

Minzheng Duan

(LAGEO, Institute of Atmospheric Physics, Chinese Academy of Sciences)

Radiative transfer and its numerical simulation is of the most important theory in atmospheric remote sensing such as temperature, humidity, aerosols and trace gases loading, and it is also a very important tool for accurate estimation of their effect on climate. In the past a few years, several methods have been developed in algorithm of radiative transfer in the atmosphere-earth system, both focusing on radiative forcing in climate and remote sensing.

To improve the computational efficiency, Wei et al. (2012) developed a combined radiative transfer model CART, which is based on DISORT by Stamnes et al.(1988).The absorption of atmospheric gases is given by a Fast Fitting Transmittance Model (FFTM), which is based on step interpolation of pre-calculated table in limited wavelengths and atmospheric profiles. A database of fitting coefficients is then created that can be used to compute narrowband transmittances for an arbitrary atmospheric profile. The CART is accurate and efficient for transmittances computation of moderate-spectral resolution, but polarization is not included.

As the advantage of polarized measurement for atmospheric aerosols, a full polarized radiative transfer model base on the successive order of scattering (SOSVRT) is developed by Duan et al. (2010),several techniques such as truncation of scattering orders, analytical Fourier decomposition of phase matrix, symmetry relationships and mutual inverse operators has been implemented to overcome the computational burdens of convergence. To improve the accuracy, a post-processing procedure is implemented to accurately interpolate the Stokes vector at arbitrary angles. The SOSVRT could be used for surfaces with both Lambertian and directional reflection, but currently only the BRDF (Bidirectional Reflection Distribution Function) model of ocean surface is implemented (Li et al, 2014). SOSVRT is accurate and much more efficient in vector radiative transfer modeling, especially

for an optical thin atmosphere, which is the most common case in polarized radiative transfer simulations. Based on adding-doubling method, He et al., (2010) expanded the RT3 (Evans and Stephens, 1991) to a coupled Atmosphere-Ocean system, and the wavy ocean surface model is implemented into this new model PCOART(He et al., 2007).

A plane-parallel atmosphere is assumed in most radiative transfer model, which is not applicable for limb sounding of atmospheric vertical profile. A simple Limb model for solving the transfer of polarized light in spherical atmosphere is developed by Geo et al., and the atmosphere is thought to be horizontal inhomogeneous.

The atmosphere is often divided into several homogeneous layers in simulations of radiative transfer in plane-parallel media. This artificial stratification introduces discontinuities in the vertical distribution of the inherent optical properties at boundaries between layers, which result in errors in the radiative transfer simulations. To investigate the effect of the vertical discontinuity of the atmosphere on radiative transfer simulations, a simple two layer model with only aerosols and molecules and no gas absorption is used. The results show that errors larger than 10% for radiances and several percent for irradiances could be introduced if the atmosphere is not layered properly (Duan et al., 2010).

Though it is not accurate, two-stream approximation is often used in the radiation processes in General Circulation Model (GCM) to reduce the time consumption. To improve the accuracy, the four-stream algorithm is introduced by Zhang and Lu (2014) in their GCM BCC\_AGCM model (Zhang and Lu, 2015) to compute the radiation process for each layer of the atmosphere, and then the two-stream algorithm is used to combine the radiation between different layers. This new algorithm improves the cold bias phenomena generally existing in the lower parts of the stratosphere above the tropics.

Horizontal visibility measured at ground meteorological stations provides information of Aerosol optical depth (Lin et al., 2014). From the 3-hourly visibility-inferred AOD over East China and the GEOS-Chem simulation, Lin et al find that the inferred AOD capture the general spatio-temporal patterns of the two

MODIS datasets with negligible mean differences and the correlation coefficients exceeds 0.9. From 33 years visibility measurements from 1980 to 2012 in Baoji, China, Xiao et al.(2014) find that The best 20% of the visibility observations in a calendar year onwards, while the worst 20% exhibits a slight increasing trend from 1997 onwards. Visibility was strongly affected by anthropogenic air pollution sources(Cao et al, 2012),resulting in an average visual range (VR) of 6.4~4.5 km. High secondary inorganic aerosol contributions (i.e.,  $\text{SO}_4^{2-}$  and  $\text{NO}_3^-$ ) were the main contributors for  $\text{VR} < 5$  km. The threshold  $\text{PM}_{2.5}$  mass concentration, corresponding to  $\text{VR} < 10$  km, was  $\sim 88 \mu\text{g m}^{-3}$ .

The total column-averaged volume mixing ratio of atmospheric carbon dioxide ( $\text{XCO}_2$ ) has been retrieved with high spectral resolution solar absorption data obtained from ground-based Fourier transform spectrometer (FTS), the DOAS method was used by Li et al. (2014) for the  $\text{XCO}_2$  measurement at Xichong Astronomical Observatory, the uncertainty of their method was about 2.0 ppm (0.51 %), while a DOAS-like method, which the ratios carefully selected between the strong and weak-absorption spectral, was used by Huo et al.(2015) retrieve the  $\text{XCO}_2$  from the ground FTS measurement of solar direct beam, their results show a good agreement with that of TCCON official algorithm. The DOAS-like algorithm reduces computational cost and less dependent on prior temperature and  $\text{H}_2\text{O}$  value than that of spectral fitting method.

Based on empirical orthogonal functions (EOF), a rapid regression algorithm for the retrieval of methane ( $\text{CH}_4$ ) profile from thermal band of Atmospheric Infrared Sounder (AIRS) (Zhang et al., 2014), the RMSE of the retrieved  $\text{CH}_4$  total column amount is less than 3% compared with that from the ground-based FTS measurement. Deng et al. (2014) developed an algorithm to derive the  $\text{CH}_4$  from the  $1.65 \mu\text{m}$  ( $5,900\text{-}6,150 \text{ cm}^{-1}$ ) and  $2.06 \mu\text{m}$  band ( $4,800\text{-}4,900 \text{ cm}^{-1}$ ) shortwave Infrared measurement, which is currently used by GOSAT, OCO and Chinese TanSAT. Validation from the GOSAT shows the retrieval errors were less than 1%

An algorithm for retrieving the surface pressure from oxygen A-band measurements was developed by Liu et al. (2014), the surface pressure and other

related atmospheric parameters such as aerosol optical depth (AOD), surface albedo, and temperature were derived through optimal estimation theory. The algorithm showed an accuracy of  $< 4$  hPa for surface pressure compared with the ground in situ measurements.

1. Cao, J., Q. Wang, J. C. Chow, J. G. Watson, X. Tie, Z. Shen, P. Wang, Z. An, Impacts of aerosol compositions on visibility impairment in Xi'an, China, *Atmospheric Environment*, 2012, 59, 559~566
2. Deng, J., Y. Liu, D. Yang, Z. Cai, CH<sub>4</sub> retrieval from hyperspectral satellite measurements in shortwave infrared: sensitivity study and preliminary test with GOSAT data, *Chinese Science Bulletin*, 2014, 59, 1499-1507.
3. Evans, K., and L. Stephens, A new polarized atmospheric radiative transfer model. *J Quant Spect Rad Trans*, 1991, 46, 413–23.
4. Gao, J., M. Duan, S. Sun, A simple limb model for solving vector radiative transfer in the horizontal inhomogeneous atmosphere, *Remote Sensing Technology and Application*, 2014, 29, 735-743. (in Chinese)
5. He, X., D. Pan, Y. Bai, Q. Zhu, F. Gong, Vector radiative transfer numerical model of coupled ocean–atmosphere system using matrix-operator method. *Sci China Ser D*, 2007, 50, 442–52.
6. He, X., Y. Bai, Q. Zhu, F. Gong, A vector radiative transfer model of coupled ocean–atmosphere system using matrix-operator method for rough sea-surface, *Journal of Quantitative Spectroscopy & Radiative Transfer* 111 (2010) 1426–1448.
7. Huo, Y., M. Duan, W. Tian, and Q. Min, A differential optical absorption spectroscopy method for XCO<sub>2</sub> retrieval from ground-based Fourier transform spectrometers measurements of the direct solar beam, *Adv. Atmos. Sci.*, accepted, 2015.
8. Li, J., C. Li, J. Mao, D. Yang, D. Wang, L. Mei, G. Shi, Y. Wang, X. Mao, *Chin. Sci. Bull.*, 2014, 59, 1536–1540.
9. Li Jiao, DuanMinzheng, Qin Jun. A Coupled Successive Order Scattering Vector

- Radiative Transfer Model For Ocean-Atmosphere System, Remote Sensing Technology and Application, 2014, 29, 181-188.
10. Lin Jintai, Donkelaar Aaron van, Xin Jinyuan, CheHuizheng, Yuesi, Clear-sky aerosol optical depth over East China estimated from visibility measurements and chemical transport modeling. Atmospheric Environment, 2014, 95, 258~267
  11. Liu Hailei, DuanMinzheng, LüDaren, Zhang Yan, Algorithm for retrieving surface pressure from hyper-spectral measurements in oxygen A-band, Chinese Science Bulletin 2014, 9, 1492-1498
  12. Wei Heli, Chen Xiuhong and Dai Congming, Combined atmospheric radiative transfer (CART) model and its applications, Infrared and Laser Engineering, 2012, 41, 3360-3366
  13. Xiao S., Wang Q., Cao J., Huang R., Chen W., Han Y., Xu H., Liu S., Zhou Y., Wang P., Zhang J., Zhan C., Long-term trends in visibility and impacts of aerosol composition on visibility impairment in Baoji, China, Atmospheric Research, 2014, 149, 88 - 95
  14. Zhang Hua, Lu Peng, Jing Xianwen. 2015. Application of two-four stream spherical harmonic expansion approximation in a global climate model. Chinese Journal of Atmospheric Sciences(in Chinese), 39, 137-144.
  15. Zhang Hua, Lu Peng, 2014. Construction of the multi-layers four-stream spherical harmonic expansion algorithm and its application to atmospheric radiative model. Acta Meteorologica Sinica(in Chinese) . 72, 1257 -1268
  16. Zhang Ying, Xiong Xiaozhen, Tao Jinhua, Yu Chao, Zou Mingmin, Su Lin, Chen Liangfu, Methane retrieval from Atmospheric Infrared Sounder using EOF-based regression algorithm and its validation, Chinese Science Bulletin, 2014, 59, 1508-1518

# Stratospheric processes and stratosphere-troposphere coupling

Jianchun Bian and Daren Lu

(LAGEO, Institute of Atmospheric Physics, Chinese Academy of Sciences)

Wen Chen

(CMSR, Institute of Atmospheric Physics, Chinese Academy of Sciences)

## **1. Stratosphere-troposphere exchange during the Asian summer monsoon**

The study on the atmospheric physical and chemical processes within the tropopause transition layer over the Asian summer monsoon region is a new emerging topic in the international atmospheric scientific community after the extensive investigation on the tropical tropopause layer (TTL). To investigate the TTL, many comprehensive in situ field campaigns have been conducted and some critical scientific advances have been made, but no effective in situ field campaigns have been planned to study the tropopause layer over the Asian summer monsoon. In 2009 summer, the Institute of Atmospheric Physics/Chinese Academy of Sciences (IAP/CAS) conducted the first combined ozone and water vapor soundings in Kunming. And from then on, IAP/CAS, together with Chinese Academy of Meteorological Sciences, has been conducting water vapor, ozone, and particle measurements with balloon-borne instruments with high accuracy. These measurements reveal some important new findings (Bian et al., 2012). The finding of the Asian tropopause aerosol layer (ATAL) from the CALIPSO measurements was supported by sounding the balloon-borne COBALD, an in situ instrument to derive particle characteristics from the backscattering signal of two wavelength light beams (455nm and 870 nm), from Kunming and Lhasa during the Asian summer monsoon (Vernier et al., 2015). Super-saturation was observed in the upper troposphere with a frequency of above 20 percent, and sometimes 150% with respect to ice was measured by balloon-borne CFH sensor, which detects the frost-point of the air directly (Bian et al., 2012). In comparison with the tropical tropopause layer, the air within the anticyclone of the Asian summer monsoon has higher (lower) water vapor

(ozone) concentration. These results will be useful for further investigating the microphysical characteristics of the cirrus in the upper troposphere, and provide the in situ evidence to the findings derived satellite-based measurements. By analysis of these measurements in the view of chemical and thermal structure, it was found that the tropopause layer over the Asian summer monsoon region shares the same structure with that over the tropics, with L-shape in the water vapor-ozone correlation scatter plot, and transition layer with a thickness of 4-5km (Pan et al., 2014).

By composite analysis, the bimodality of the upper tropospheric anticyclone of the Asian summer monsoon has an impact on the distribution of chemical constituents in the UTLS region (Yan et al., 2011). For the Iranian Plateau mode, the tropospheric tracers (such as CO and water vapor) exhibited a positive anomaly over the Iranian Plateau and a negative anomaly over the Tibetan Plateau, whereas the stratospheric tracer (ozone) exhibited a negative and a positive anomaly over the Iranian Plateau and the Tibetan Plateau, respectively. For the Tibetan Plateau mode, however, the distribution of the anomaly was the reverse of that found for the chemical species in the UTLS region. Furthermore, the locations of the extrema within the anomaly seemed to differ across chemical species.

The formation of the summertime total ozone valley over the Tibetan plateau was revealed from the measurements (SAGE II and OMI data), and it was pointed that the Asian summer monsoon and air column variations are the two main causes (Bian et al., 2011). Satellite observations of ozone profiles show that ozone concentrations over the ASM region have lower values in the upper troposphere and lower stratosphere (UTLS) than over the non-ASM region, which is caused by frequent convective transport of low-ozone air from the lower troposphere to the UTLS region combined with trapping by the South Asian High. In addition, along the same latitude, total ozone changes identically with variations of the terrain height, showing a high correlation with terrain heights over the ASM region, which includes both the Tibetan and Iranian plateaus.

The Asian summer monsoon (ASM) anticyclone during boreal summer has persistent maxima in carbon monoxide (CO). This enhancement is due to the upward

transport of air with high CO from the planetary boundary layer (PBL), and confinement within the anticyclonic circulation (Yan & Bian, 2015). A source sensitivity experiment was performed using the Weather Research and Forecasting (WRF) with chemistry model (WRF-Chem), and it was found that the CO within the ASM anticyclone mostly comes from India, while the contribution from East China is insignificant. This difference is mainly caused by the different transportation mechanisms. Over the India subcontinent, CO transportation is primarily affected by convection. However, the CO transportation over East China is affected by deep convection and large-scale circulation, with little upward transport to the anticyclone.

## **2. Anomaly in the stratospheric circulation and its relation to the weather and climate in the troposphere**

An extremely cold event over the boreal middle and high latitude region during 2009 December as a typical case, the relationship between the abnormal cold winter weather and the stratospheric circulation anomaly was investigated, it was shown that the stratospheric dynamical process played an important role in the occurrence of the extremely cold event at the lower levels (Wang & Chen, 2010). The downward propagation of the stratospheric circulation anomaly occurs not only during some strong anomaly events, but also during some moderate stratospheric polar vortex, which implies the complication in the stratosphere-troposphere coupling processes.

From the analysis of the monsoon tendency index (MTI) of the East Asian monsoon index after 2000, it was shown that the winter monsoon setup has been postponed in autumn, while the setup has quickened in early winter (Wei et al., 2011). A north-south seesaw of temperature tendency change in China can be observed in December and February, which may be related to large-scale circulation changes in the stratosphere, characterized by a polar warming in mid winter and polar cooling in early spring. This linkage is possibly caused by the dynamical coupling between stratosphere and troposphere, via the variation of planetary wave activities

Analysis of the temporal and spatial relationship between ENSO and the extratropical stratospheric variability in the Northern Hemisphere shows that there exists a negative correlation between ENSO and the strength of the polar vortex, but

the maximum correlation is found in the next winter season after the mature phase of ENSO event, rather than in the concurrent winter (Ren et al., 2012). Specifically, the stratospheric polar vortex tends to be anomalously warmer and weaker in both the concurrent and the next winter season following a warm ENSO event, and vice versa. However, the polar anomalies in the next winter are much stronger and with a deeper vertical structure than that in the concurrent winter.

1. Bian, J., R. Yan, H. Chen, D. Lu, and S. T. Massie, 2011: Formation of the summertime ozone valley over the Tibetan Plateau: The Asian summer monsoon and air column variations. *Adv. Atmos. Sci.*, 28(6), 1318-1325, doi:10.1007/s00376-011-0174-9.
2. Bian, J., L. L. Pan, L. Paulik, H. Vömel, H. Chen, and D. Lu (2012), In situ water vapor and ozone measurements in Lhasa and Kunming during the Asian summer monsoon, *Geophys. Res. Lett.*, 39, L19808, doi:10.1029/2012GL052996.
3. Pan, L. L., L. C. Paulik, S. B. Honomichl, L. A. Munchak, J. Bian, H. B. Selkirk, and H. Vömel (2014), Identification of the tropical tropopause transition layer using the ozone-water vapor relationship, *J. Geophys. Res. Atmos.*, 119, doi:10.1002/2013JD020558.
4. Ren, R. C., M. Cai, C. Y. Xiang, and G. X. Wu, 2012: Observational evidence of the delayed response of stratospheric polar vortex variability to ENSO SST anomalies. *Clim. Dyn.*, 38, 1345-1358, doi:10.1007/s00382-011-1137-7.
5. Vernier, J.-P., T. D. Fairlie, M. Natarajan, F. G. Wienhold, J. Bian, B. G. Martinsson, S. Crumeyrolle, L. W. Thomason, and K. M. Bedka (2015), Increase in upper tropospheric and lower stratospheric aerosol levels and its potential connection with Asian pollution, *J. Geophys. Res. Atmos.*, 120, 1608–1619, doi:10.1002/2014JD022372.
6. Wang, L., and W. Chen, 2010: Downward Arctic Oscillation signal associated with moderate weak stratospheric polar vortex and the cold December 2009. *Geophys. Res. Lett.*, 37, L09707, doi:10.1029/2010gl042659.
7. Wei, K., W. Chen, and W. Zhou, 2011: Changes in the East Asian Cold Season

since 2000. *Adv. Atmos. Sci.*, 28, 69-79, doi:10.1007/s00376-010-9232-y.

8. Yan, R., J. Bian, and Q. Fan, 2011: The impact of the South Asia High Bimodality on the chemical composition of the upper troposphere and lower stratosphere, *Atmos. Oceanic Sci. Lett.*, 4, 229–234.
9. Yan, R. C., and J. C. Bian, 2015: Tracing the boundary layer sources of carbon monoxide in the Asian summer monsoon anticyclone using WRF-Chem. *Adv. Atmos. Sci.*, 32(7), 943–951, doi: 10.1007/s00376-014-4130-3.